The farinfrared vibration–rotation–tunneling spectrum of the water tetramerd8

J. D. Cruzan, M. G. Brown, K. Liu, L. B. Braly, and R. J. Saykally

Citation: The Journal of Chemical Physics **105**, 6634 (1996); doi: 10.1063/1.471977
View online: http://dx.doi.org/10.1063/1.471977
View Table of Contents: http://scitation.aip.org/content/aip/journal/jcp/105/16?ver=pdfcov
Published by the AIP Publishing

The far-infrared vibration–rotation–tunneling spectrum of the water tetramer-*d*8

J. D. Cruzan, M. G. Brown, K. Liu, L. B. Braly, and R. J. Saykally
Department of Chemistry, University of California at Berkeley, Berkeley, California 94720

(Received 11 June 1996; accepted 22 July 1996)

The far-infrared vibration–rotation–tunneling spectrum of $(D_2O)_4$ has been measured in the spectral region near 2.04 THz. Observation of additional transition doublets with a constant 5.6 MHz spacing in a parallel (*c*-type) spectrum extends the first detailed study of this cluster [Science **271**, 59 (1996)]. Three possibilities are explored for the origin of this small splitting: tunneling between degenerate equilibrium structures via facile torsional motions analogous to those observed in the water trimer, tunneling between nondegenerate structural frameworks, and tunneling made feasible only through excitation of a specific vibrational coordinate. The degenerate tunneling scheme best accounts for the spectral features, although the precise dynamics responsible for the observed spectral features cannot be uniquely established from the present data. A further doubling of spectral features, observed only in the $K=2$ manifold of transitions for $J\geqslant 3$, is symmetric about the unperturbed symmetric top energy levels and shows an approximate J^2 dependence of the spacing. The origin of these additional splittings, which are shown to be present in both upper and lower vibrational states of the spectrum, is likely to be due to an interaction between overall rotational angular momentum and the type of internal motion (''pseudorotation'') that gives rise to a manifold of low energy states in water trimer. The measured interoxygen separations in $(D_2O)_n$ $(n=2,3,4,5)$ are analyzed in order to quantify the contribution of many-body forces in bulk water. An exponential contraction of this property toward the value found in ordered ice is observed. © *1996 American Institute of Physics.* [S0021-9606(96)02540-8]

I. INTRODUCTION

In an effort to understand the complicated behavior of condensed water on a molecular scale, much effort has been undertaken to study small isolated aggregates of water molecules.[1] The water dimer has proven an exceptional experimental and theoretical challenge in this regard for more than two decades.[2] Detailed experimental studies of larger water clusters have only become possible within the last few years. The principal aim of these studies has been to extract accurate, detailed representations of the multidimensional intermolecular potential energy surfaces (IPS) of $(H_2O)_n$, including both pairwise and cooperative (many-body) interactions,[3] and to quantify the nature of hydrogen bond formation–bond breaking dynamics.

Classical simulations[4–6] have characterized liquid water as a continuous hydrogen bonded network of closed polygons dominated by 5–8 membered rings. Belch and Rice[4] have shown that relaxation of the hydrogen bond network is slow compared to the time scale for intermolecular vibrations inside a localized cluster, which correspond to monomer translational and librational motions. Water polygons have also been associated with aqueous solvation processes via clathrate formation[7–9] and by the formation of hydrophobic group ''caps'' in several studies of biological macromolecules.[10,11] In the latter case, these polygons have been shown to be localized over the long time scales of x-ray diffraction experiments.

Far-infrared (FIR) vibration–rotation–tunneling (VRT) spectroscopy has emerged as a valuable tool[1,12] for measuring both the bound intermolecular vibrations and rotation–tunneling fine structure of weakly bound systems. The ground states and a few intermolecular vibrational modes of small water clusters[13–17] and other important prototypical systems[18,19] have now been examined in detail using this method. FIR-VRT spectra and other data have been inverted to produce spectroscopically accurate IPS for such weakly bound clusters as $Ar\cdot H_2O$,[20] $Ar\cdot NH_3$,[21] $(HCl)_2$,[22] and $(NH_3)_2$.[23] Recent work[24] on $Ar_2\cdot HCl$ has used Hutson's accurate $Ar\cdot HCl$ potential in conjunction with VRT data[18,25,26] on the ternary complex to quantify the nature of cooperative forces in that cluster. Coupled with recent advances in computational methodology,[27] FIR-VRT studies have now put a detailed determination of the six-dimensional water dimer IPS within reach.

Pugliano and Saykally[28] reported the first detailed experimental study of the water trimer using FIR-VRT spectroscopy. Since then considerable experimental[15,29–32] and theoretical[33–39] work has augmented that initial study. Recently, FIR-VRT spectra of the perdeuterated forms of the water tetramer[16] and pentamer[17] were reported. Vibrationally averaged structures for both were found to agree with theoretically predicted cyclic, quasiplanar equilibrium structures, analogous to that of the trimer (Fig. 1). A three-dimensional cage form of the water hexamer has been characterized as well.[40] With these data one can now begin to examine in quantitative detail the effects of hydrogen bond cooperativity on water cluster structures and binding energies. The average interoxygen separation (R_{OO}) is an experimentally accessible measure of the degree of hydrogen bond cooperativity in cyclic water clusters. In a recent study of cooperative forces

 0021-9606/96/105(16)/6634/11/$10.00

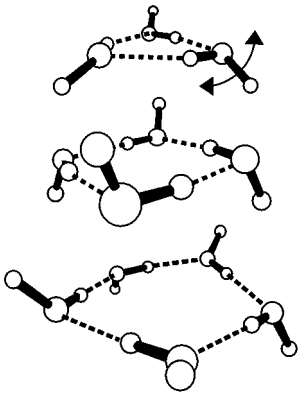

FIG. 1. Calculated (Ref. 38) cyclic, quasiplanar equilibrium structures of the water trimer, tetramer, and pentamer. The illustrated ''flipping'' coordinate is a key component of the observed VRT dynamics in the water trimer and pentamer, and is likely to be an important component of the tetramer dynamics as well. The water tetramer equilibrium structure has S_4 point group symmetry and is therefore rigorously a symmetric top by symmetry. Note that alternative quasiplanar structures have been predicted to lie near in energy to the S_4 structure (see the text). The water trimer and pentamer also exhibit symmetric top VRT spectra but must be ''dynamical'' symmetric rotors due to the flipping motion which vibrationally averages the unbound proton positions to lie within the plane of the oxygen atoms.

in water, Xantheas[38] predicted an exponential decrease in R_{OO} with increasing cluster size for cyclic ($n=3,4,5$) water clusters, converging to the bulk (ordered ice) value by $n=5$ or 6, for rotationally cold clusters. The growing body of VRT data on larger water clusters now allows direct comparison to such theoretical results.

In the case of the water dimer, all possible hydrogen bond network rearrangements (HBNR) among equivalent minima on the six-dimensional IPS have been observed to give rise to spectral effects.[2] Furthermore, it is a relatively straightforward matter to assign the splittings based upon approximate barriers to the respective interconversions. The water tetramer presents a more challenging problem. For larger water clusters, the extra stabilization energy gained from hydrogen bond network cooperativity, and relaxation of the hydrogen bond strain present in smaller rings, appears to restrict the observable HBNR dynamics. The characteristic quartet tunneling splitting patterns observed in both $(H_2O)_3$ and $(D_2O)_3$ FIR-VRT spectra, arising from an exchange of the bound and free protons of one monomer (''bifurcation'' or ''donor'' tunneling), have not been observed in either the tetramer or pentamer spectra. From group theoretical arguments, these motions might be expected to give rise to as many as $n+1$ resolved spectral components. Coupled with the increasing complexity of the multidimensional IPS describing larger systems, the HBNR dynamics responsible for spectral splittings have become more difficult to specify.

Theoretical calculations[38,41–54] of the properties of small ($n<20$) water clusters have so far indicated two structural regimes. Clusters smaller than the hexamer appear to have unique equilibrium structures, corresponding to quasiplanar rings, as observed for the trimer, tetramer, and pentamer. A monotonic decrease in hydrogen bond strain with ring size is predicted to increase the per monomer binding energy, culminating with the pentamer, where near linear hydrogen bonding angles produce the minimum geometric strain. Indeed, the stable cyclic pentamer is the essential building block of water clathrate structures.[8] In each case ($n=3–5$), cyclic structures are significantly favored over three-dimensional structures. In contrast, Jordan and co-workers[54] have calculated 44 low energy water hexamer structures, including cyclic, and two- and three-dimensional forms, lying within 3.2 kcal mol^{-1} of the global minimum (less than one hydrogen bond stabilization energy). Other *ab initio* calculations[41,44–46,55] have produced similar results. Both cases—clusters with isolated cyclic structures and larger clusters wherein the zero-point energies may well be above the barriers to rearrangement between structurally distinct IPS minima—present a challenge to the ''usual'' methods of analyzing the consequences of hydrogen bond network rearrangements in the VRT spectra.

In this paper, we present a detailed analysis of the water tetramer, built on an augmented set of measurements of a VRT spectrum centered near 2.0 THz. Due to several instrumental improvements, the number of observed $(D_2O)_4$ VRT transitions reported in Ref. 16 has been doubled. Three scenarios are described which could lead to the observed tunneling doublets. A vibrational assignment is given in light of recent *ab initio* harmonic frequency calculations, and trends in the values of R_{OO}, the vibrationally averaged interoxygen separation estimated from the data, are analyzed in terms of their implications on the magnitude of cooperative forces in bulk water. An additional doubling of spectral features, observed exclusively in the $K=2$ manifold, is interpreted in terms of a coriolis-type coupling of internal motions and overall rotational angular momentum, similar to that which has been proposed for the water trimer.[34,36]

II. EXPERIMENT AND RESULTS

The tunable FIR laser sideband spectrometers used in this work have been described in detail elsewhere,[56] therefore only the details relevant to this work will be given here. Water clusters were formed in supersonic expansions of D_2O (Cambridge Isotopes, 99.96% purity) seeded in Ar, Ne (70% with He), or He. Two nozzle expansion sources were used in this work. The first was a 10 cm$\times$0.0013 cm continuously operated planar nozzle[57] used with typical backing pressures of 1 atm. The second, a pulsed planar jet of our own design[58] with similar dimensions, allowed for operation at higher (2–6 atm) backing pressures. Tenfold signal-to-noise ratio enhancements were realized using the pulsed jet over the cw source. The increase, when scaled for the loss ($\sim$factor of 100) in detection duty cycle inherent in a pulsed beam detection scheme, indicates that the pulsed nozzle is a superior source of clusters, presumably due to the increase in collision frequency in the cluster forming region of the jet, which scales with the stagnation pressure. Two optically pumped FIR laser transitions were used to record all of the data in this work: 2027.7526 GHz (CH_3NH_2) and 2058.1418 GHz (CH_3OD).

The optical multipass design of Herriott[59] has been

implemented in the spectrometers used in this work and has been found to be quite satisfactory at refocusing the divergent FIR sideband radiation over many passes through the jet. The expansions in this work were typically probed by multipassing the FIR laser 22 times, 0.5–2 cm in front of the nozzle aperture yielding absorption path lengths of over 2 m, a threefold improvement over the previous design.[60]

As a result of these improvements, the number of $(D_2O)_4$ transitions observed was doubled from that of Ref. 16. A total of 113 FIR-VRT transitions belonging to a parallel ($\Delta K=0$) band of a symmetric oblate rotor have now been recorded in the spectral region near 2.04 THz (68 cm^{-1}). The observed transitions are listed in Table I. Each transition was observed as a doublet of lines with nearly equal intensity and spaced by 5.6 ± 0.1 MHz with no J or K dependence of the spacing, indicative of tunneling splittings in either or both the vibrational ground or excited states. Figure 2 shows the observed spectrum and representative doublet transitions recorded with the pulsed nozzle source.

In order to confirm the identity of the absorber, carrier gas and isotopic substitution experiments were performed. Because the signals were observed in expansions of D_2O seeded in He, Ne, or Ar, the cluster was assumed to contain only D_2O. The number of monomers was determined by measuring the intensities of several signals as a function of D_2O concentration in an H_2O+D_2O mixture. As described previously,[16,28] several mixtures were analyzed and the relative intensities of a few doublet transitions were least-squares fit to the expression $\ln(I_{\mathrm{rel}}) = 2n\ \ln(\chi_{D_2O})$, where I_{rel} is the relative intensity, n is the number of water monomers in the cluster, and χ_{D_2O} is the mole fraction of D_2O in the mixture. The slope of a linear plot of several data points from such an analysis has yielded reliable measurements of n for $(D_2O)_n$, $n=2$, 3, 5, and $(H_2O)_n$, $n=2$, 3, 6, as well as a variety of mixed trimer isotopomers.[32] Interestingly, these results seem to indicate that, within the ability of the experiment to precisely measure intensity changes, kinetic isotope effects do not play a significant role in the formation of small water clusters in a free expansion. The most significant evidence for the origin of the spectrum lies in the fitted rotational parameters, which are precise to within a few megahertz and cannot be explained by any other absorber or any reasonable impurity.

The VRT data were least-squares fit to the simple symmetric top energy level expression

$$E_{J,K}=\overline{B}J(J+1)+(C-\overline{B})K^2 - D_J J^2(J+1)^2-D_{JK}J(J+1)K^2. \quad (1)$$

Each datum in the fit was the average of the two tunneling doublet line positions. The $K=2$ transitions, for which additional doubling of the lines was observed, were included in initial fits by averaging the split doublet centers (i.e., by averaging the four observed line positions). Table II shows the rotational and centrifugal distortion parameters obtained from the regression to Eq. (1) using the averaged $K=2$ line positions. Some of the $K=2$ R-branch splittings are illustrated in Fig. 3, and the splittings are given in Table III.

TABLE I. The observed VRT transitions (MHz). Residuals (observed–calculated transitions) are from the least-squares fit of the data to Eq. (1), as described in the text. Missing low J transitions are due to small laser coverage gaps. Each frequency is the average of a 5.6 MHz tunneling doublet or of two in the case of the $K=2$ transitions.

$J'_{K'}\leftarrow J''_{K''}$	Freq./MHz	Residual	$J'_{K'}\leftarrow J''_{K''}$	Freq./MHz	Residual
$7_0\leftarrow8_0$	1 984 117.6	0.1	$11_{10}\leftarrow11_{10}$	2 032 730.0	−0.5
$7_1\leftarrow8_1$	1 984 101.6	0.0			
$7_2\leftarrow8_2$	1 984 054.1	0.4	$4_2\leftarrow4_2$	2 032 866.0	−3.8
$7_3\leftarrow8_3$	1 983 974.8	0.9	$5_3\leftarrow5_3$	2 032 913.0	−0.4
$7_4\leftarrow8_4$	1 983 861.8	−0.4	$6_4\leftarrow6_4$	2 032 948.0	−2.0
$7_5\leftarrow8_5$	1 983 719.4	0.8	$7_5\leftarrow7_5$	2 032 979.0	−0.6
			$8_6\leftarrow8_6$	2 033 002.0	−0.2
$6_0\leftarrow7_0$	1 990 100.1	0.2	$9_7\leftarrow9_7$	2 033 017.0	−0.8
$6_1\leftarrow7_1$	1 990 084.2	0.2	$10_8\leftarrow10_8$	2 033 027.0	0.7
$6_2\leftarrow7_2$	1 990 033.6	−2.6			
$6_3\leftarrow7_3$	1 989 957.7	1.1	$4_1\leftarrow4_1$	2 032 913.0	−3.9
$6_4\leftarrow7_4$	1 989 846.6	1.5	$5_2\leftarrow5_2$	2 032 991.0	−0.8
$6_5\leftarrow7_5$	1 989 703.9	2.1			
$6_6\leftarrow7_6$	1 989 525.5	−1.0	$1_1\leftarrow0_0$	2 038 874.2	2.4
$5_0\leftarrow6_0$	1 996 108.3	0.2	$2_0\leftarrow1_0$	2 045 081.2	1.8
$5_1\leftarrow6_1$	1 996 092.5	0.2	$2_1\leftarrow1_1$	2 045 065.0	1.2
$5_2\leftarrow6_2$	1 996 042.0	0.3	$7_0\leftarrow6_0$	2 076 472.4	0.0
$5_3\leftarrow6_3$	1 995 965.6	−2.5	$7_1\leftarrow6_1$	2 076 457.2	0.2
$5_4\leftarrow6_4$	1 995 854.3	0.6	$7_2\leftarrow6_2$	2 076 410.9	0.2
$5_5\leftarrow6_5$	1 995 711.3	0.5	$7_3\leftarrow6_3$	2 076 334.2	0.6
			$7_4\leftarrow6_4$	2 076 226.2	0.6
$4_0\leftarrow5_0$	2 002 142.2	0.3	$7_5\leftarrow6_5$	2 076 087.6	0.8
$4_1\leftarrow5_1$	2 002 126.3	0.3	$7_6\leftarrow6_6$	2 075 917.8	0.7
$4_2\leftarrow5_2$	2 002 078.9	0.5			
$4_3\leftarrow5_3$	2 002 000.6	1.5	$8_0\leftarrow7_0$	2 082 820.2	0.0
$4_4\leftarrow5_4$	2 001 889.0	0.9	$8_1\leftarrow7_1$	2 082 804.8	−0.1
			$8_2\leftarrow7_2$	2 082 758.7	0.0
$3_1\leftarrow4_1$	2 008 184.6	−0.7			
			$8_3\leftarrow7_3$	2 082 681.7	−0.1
$2_0\leftarrow3_0$	2 014 285.6	0.0	$8_4\leftarrow7_4$	2 082 574.2	0.1
$2_1\leftarrow3_1$	2 014 269.8	0.0	$8_5\leftarrow7_5$	2 082 435.7	0.1
$2_2\leftarrow3_2$	2 014 222.5	0.1	$8_6\leftarrow7_6$	2 082 226.5	0.1
			$8_7\leftarrow7_7$	2 082 066.1	−0.3
$1_1\leftarrow1_1$	2 032 694.0	−3.1			
$2_2\leftarrow2_2$	2 032 704.0	5.1	$9_0\leftarrow8_0$	2 089 190.2	−0.4
$3_3\leftarrow3_3$	2 032 693.0	−0.7	$9_1\leftarrow8_1$	2 089 175.1	−0.1
$4_4\leftarrow4_4$	2 032 682.0	0.4	$9_2\leftarrow8_2$	2 089 129.1	−0.1
$5_5\leftarrow5_5$	2 032 662.0	−0.5	$9_3\leftarrow8_3$	2 089 052.3	−0.2
$6_6\leftarrow6_6$	2 032 636.0	−0.4	$9_4\leftarrow8_4$	2 088 944.9	−0.1
$7_7\leftarrow7_7$	2 032 603.0	−0.2	$9_5\leftarrow8_5$	2 088 806.6	−0.3
$8_8\leftarrow8_8$	2 032 564.0	0.6	$9_6\leftarrow8_6$	2 088 638.0	−0.1
$9_9\leftarrow9_9$	2 032 516.0	−0.5	$9_7\leftarrow8_7$	2 088 438.4	−0.3
			$9_8\leftarrow8_8$	2 088 207.7	−0.8
$10_{10}\leftarrow10_{10}$	2 032 462.0	−0.6			
$11_{11}\leftarrow11_{11}$	2 032 402.0	0.2	$3_0\leftarrow2_0$	2 051 310.8	−0.2
$12_{12}\leftarrow12_{12}$	2 032 334.0	0.0	$3_1\leftarrow2_1$	2 051 295.7	0.3
$13_{13}\leftarrow13_{13}$	2 032 260.0	0.8	$3_2\leftarrow2_2$	2 051 248.5	−0.2
$14_{14}\leftarrow14_{14}$	2 032 178.0	0.4			
$15_{15}\leftarrow15_{15}$	2 032 089.0	0.1	$4_0\leftarrow3_0$	2 057 565.9	−0.5
$16_{16}\leftarrow16_{16}$	2 031 993.0	−0.3	$4_1\leftarrow3_1$	2 057 550.3	−0.5
$17_{17}\leftarrow17_{17}$	2 031 891.0	0.2	$4_2\leftarrow3_2$	2 057 503.7	−0.5
$18_{18}\leftarrow18_{18}$	2 031 781.0	−0.3	$4_3\leftarrow3_3$	2 057 423.1	−3.4
$19_{19}\leftarrow19_{19}$	2 031 665.0	0.1			
			$5_0\leftarrow4_0$	2 063 844.5	−0.7
$3_2\leftarrow3_2$	2 032 771.0	−1.	$5_1\leftarrow4_1$	2 063 829.1	−0.62
$4_3\leftarrow4_3$	2 032 791.0	−0.4	$5_2\leftarrow4_2$	2 063 783.9	0.7
$5_4\leftarrow5_4$	2 032 802.0	−1.6	$5_3\leftarrow4_3$	2 063 705.1	−0.6
$6_5\leftarrow6_5$	2 032 812.0	3.1	$5_4\leftarrow4_4$	2 063 595.9	−1.2
$9_8\leftarrow9_8$	2 032 781.0	−1.8			
$10_9\leftarrow10_9$	2 032 759.0	−1.1	$6_0\leftarrow5_0$	2 070 148.9	1.6

TABLE I. (*Continued*.)

$J'_{K'} \leftarrow J''_{K''}$	Freq./MHz	Residual	$J'_{K'} \leftarrow J''_{K''}$	Freq./MHz	Residual
$6_1 \leftarrow 5_1$	2 070 133.3	1.4	$10_2 \leftarrow 9_2$	2 095 521.4	−0.4
$6_2 \leftarrow 5_2$	2 070 086.8	1.3	$10_3 \leftarrow 9_3$	2 095 445.3	0.0
$6_3 \leftarrow 5_3$	2 070 009.2	1.1	$10_4 \leftarrow 9_4$	2 095 338.2	0.0
			$10_5 \leftarrow j9_5$	2 095 200.6	0.1
$6_4 \leftarrow 5_4$	2 069 901.2	1.3	$10_6 \leftarrow 9_6$	2 095 032.5	0.4
$6_5 \leftarrow 5_5$	2 069 762.2	1.5	$10_7 \leftarrow 9_7$	2 094 833.5	0.3
			$10_8 \leftarrow 9_8$	2 094 603.7	0.0
$10_0 \leftarrow 9_0$	2 095 583.2	0.2	$10_9 \leftarrow 9_9$	2 094 344.3	0.8
$10_1 \leftarrow 9_1$	2 095 567.7	0.0			

TABLE II. Rotational and centrifugal distortion parameters (in MHz) obtained from least-squares fit of the data in Table I to (1). The vibrational band origin is $\nu_0 = 67.8031\ \text{cm}^{-1}$.

Constant/MHz	
ν_0	2 032 688.38(33)
$A'' = B''$	3 079.512(36)
D''_J	0.0089(04)
D''_{JK}	−0.0177(07)
$A' = B'$	3 091.726(31)
D'_J	0.0092(03)
D'_{JK}	−0.0181(06)
$C' - C''$	−3.4771(67)

Removal of the $K=2$ transitions from the fit had no effect on the rotational or centrifugal distortion constants to within the uncertainties given in Table II, therefore it was assumed that the splitting was symmetric about the unperturbed $K=2$ VRT levels. Additionally, the observation that the P- and R-branch spacings were different as a function of lower and upper state J (Fig. 4) was taken as evidence that this splitting occurred in both upper and lower vibrational states. Because the compact Q-branch region of the spectrum was congested (Fig. 2), and because the $K=2$ Q-subbranch intensities decay rapidly as a function of J, it is unclear whether such splittings were present in Q-branch transitions. Trial fits of the $K=2$ data were performed by assuming a symmetric splitting about the unperturbed levels given by

$$E^{\pm}_{J,K=2} = E_{J,K=2} \pm \beta[J(J+1)]^{\alpha}, \tag{2}$$

where $E^{\pm}_{J,K=2}$ are the upper and lower components of the perturbation doublet, β is an adjustable parameter, and α was set to values of 1 and 1/2. The transitions were weighted by the squared reciprocal of the spectral uncertainty (2 MHz) while the splittings themselves (differences in transition frequencies) were included, but weighted by an uncertainty of 500 kHz or roughly one-half a linewidth (~1 MHz full width at half-maximum, Doppler limited). Such small splittings are not susceptible to the long term instrumental drift that causes the larger uncertainty of more separated lines. Fits assuming all possible combinations of selection rules, i.e., those for which the observed splittings would be the sum of or the difference between the upper and lower state $K=2$ doublets, were performed. The best results, those which produced the smallest residuals and most well-determined values of β, were obtained by fitting to Eq. (2) with $\alpha=1$ and assuming a selection rule scheme for which the observed splitting reflects the sum of the upper and lower state $K=2$ doublet levels. This fit yielded $\beta = 0.025 \pm 0.003$ and 0.063 ± 0.004

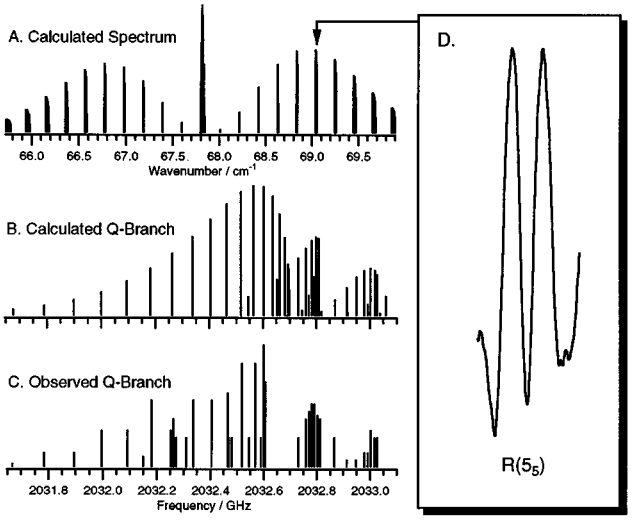

FIG. 2. (A) The $(D_2O)_4$ spectrum calculated from the measured rotational parameters (Table II). A Boltzmann rotational temperature of 5 K was used and the resulting intensity envelope was modified with symmetric top line strength (Hönl–London) factors. (B) Blowup of the compact Q-branch region in (A). (C) Experimentally observed Q branch. (D) A typical 5.6 MHz tunneling doublet transition ($6_5 \leftarrow 5_5$) recorded with the pulsed planar nozzle described in the text.

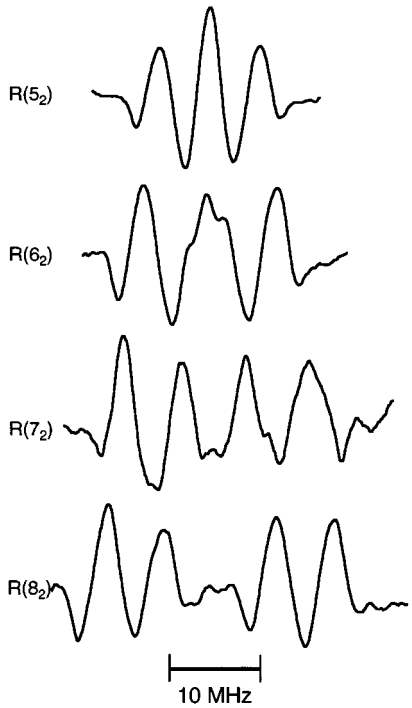

FIG. 3. Additional splitting of the $K=2$ R-branch transitions, $R(5)-R(8)$. The additional splitting could either be due to a coriolis-type interaction of internal torsional motions with the overall rotation or to quantum tunneling between nonstructurally degenerate minima on the tetramer IPS.

TABLE III. The $K=2$ splittings (MHz). The uncertainty in these splittings is approximately 500 kHz (see the text).

Transition	Splitting/MHz
3←2	0.0
4←3	1.0
5←4	3.0
6←5	5.4
7←6	8.2
8←7	12.0
9←8	16.8
4←5	2.9
5←6	5.4
6←7	7.0
7←8	11.8

MHz for the lower and upper states, respectively, although the resultant fit residuals were, on average, twice those of the initial fit to Eq. (1).

III. STRUCTURAL ANALYSIS

The moments of inertia along the symmetric top symmetry axis (the C inertial axis of an oblate rotor) cannot be determined separately from the transitions in a parallel band; transitions with $\Delta K=\pm 1$ are necessary to fix the absolute values of those parameters. Only the difference between the upper and lower state C constants could be determined from the fit of the VRT data to Eq. (1). Relative transition intensities, however, are dependent upon the magnitude of the C constant in the lower state and can therefore provide a good estimate of C''. A strategy for estimating a C constant would be to determine the experimental rotational temperature using a closely spaced $\Delta K=0$ Q-branch progression, where the relative energies do not depend upon C, then fit the strong $J''=K''$ progression, characteristic of an oblate rotor spectrum, to a Boltzmann distribution using the measured temperature and appropriate symmetric top line strength (Hönl–London) factors. This strategy has proven moderately successful in the recent analysis of a $(D_2O)_5$ spectrum.[61] Unfortunately, in the tetramer spectrum any single $\Delta K=0$ Q-branch progression is short and does not yield as precise an estimate of the rotational temperature as a longer progression might. Fits of the $K=1$ and $K=3$ Q-subbranch relative intensities, which are also dependent on fluctuations and variations of the FIR laser power, to a Boltzmann distribution yield a rotational temperature of $T_{\rm rot}=5\pm 1$ K. Fits of the $J=K$ Q-branch progression to this temperature range show a steep dependence on $T_{\rm rot}$, and yield a best estimate of $C=1500\pm 250$ MHz. Nevertheless, this value is consistent with theoretical predictions[38] that $C\approx B/2$.

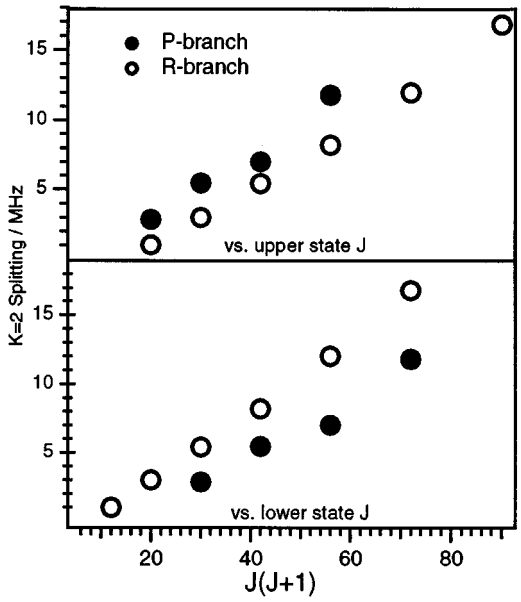

FIG. 4. Plots of the $K=2$ splittings (see Table III) vs $J(J+1)$ for both lower and upper state rotational quantum numbers J. Since the P- and R-branch splittings lie on different lines, the splittings must occur in both upper and lower vibrational states.

Interoxygen separations were estimated for the tetramer as well as the trimer and pentamer by assuming the *ab initio* monomer angular orientations of Xantheas and Dunning,[38] and varying the distance of each water molecule from the center of mass of the cluster until the resulting $A=B$ value matched the measured value. In principle, the currently available VRT data alone are insufficient to accurately determine the interoxygen separations in either trimer, tetramer, or pentamer, particularly since an experimental C rotational constant is not yet available for the latter two. However, the data for all three clusters strongly support the *ab initio* minimum energy structures when the effects of vibrational averaging (predominantly in the facile ''flipping'' coordinate) are taken into account. Theoretically calculated structural details (e.g., monomer orientations) can then aid in constraining some of the geometrical degrees of freedom. Since the rotational constants are much more sensitive to the relative oxygen positions than to the orientations of the individual water monomers about their respective centers of mass, it is reasonable to simply vary the monomer coordinates while preserving the *ab initio* monomer orientations to obtain an average $R_{\rm OO}$ estimate. The results of such calculations for the tetramer and pentamer yield $R_{\rm OO}$ values of 2.78 and 2.75 Å, respectively. Liu[30] has recently performed a Monte Carlo simulation of the water trimer using the diffusion Monte Carlo constrained wave functions of Gregory and Clary[33] to determine a vibrationally averaged $R_{\rm OO}$ value consistent with the measured rotational constants of the $(D_2O)_3$ band at 98 cm^{-1}. This more rigorous treatment of the average geometry sampled by the experiment yielded a value of $R_{\rm OO}=2.85$ Å for the trimer. Figure 5 shows a comparison of the *ab initio* and experimental trends in $R_{\rm OO}$ and $R_{\rm cm}$ as a function of cluster size. The trimer value of $R_{\rm OO}$ is strongly supported by more recent work on isotopically mixed trimers.[30,32]

As shown by Xantheas,[38] $R_{\rm OO}$ can be modeled to follow an exponential contraction with cluster size, which can be given by

$$R^{(n)}=R^{(\infty)}+Ae^{-Cn}. \tag{3}$$

Here $R^{(n)}$ is the interoxygen separation for cluster $(H_2O)_n$,

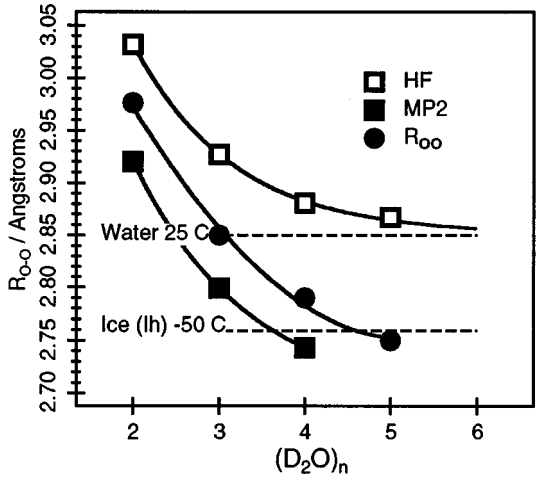

FIG. 5. Comparison of theoretical (Ref. 38) and experimental values of R_{OO}, the average interoxygen separation of water dimer, trimer, tetramer, and pentamer. The methods of calculating R_{OO} and R_{cm} are outlined in the text. Solid lines are the results of fits of Eq. (3) to the trends.

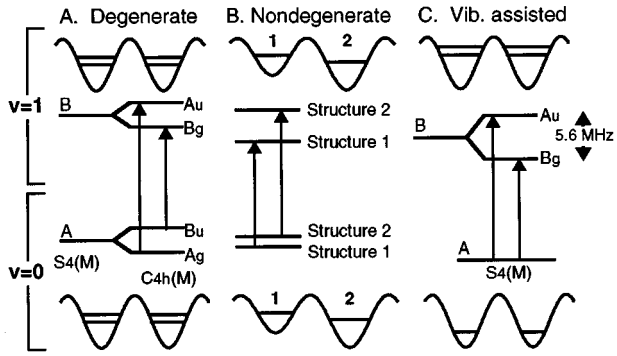

FIG. 6. Three possible scenarios which could explain the 5.6 MHz tunneling splitting observed in the $(D_2O)_4$ VRT spectrum. (A) Degenerate rearrangements occur in both the upper and lower vibrational states. Tunneling splittings are the sum or difference of upper and lower state splittings. (B) Tunneling between IPS minima supporting nondegenerate frameworks. This type of tunneling is not likely to give rise to splittings constant as a function of rotation. (C) Tunneling possible through excitation in a given vibrational coordinate which effectively lowers a barrier to degenerate rearrangement. In this case the observed spectral splitting is the energy level splitting in the upper vibrational state.

$R^{(\infty)}$ is the bulk (ordered ice) separation, and C and A are adjustable parameters. Given that the theoretical results represent the equilibrium separation, while the measured separations are vibrationally averaged, only the trends toward the bulk value can be compared. Kim and co-workers[62] have shown that no less than the MP2 level of *ab initio* calculation, with large basis sets, is required to reproduce the experimentally observed properties of the water dimer, including the dipole moment. Therefore it is appropriate to compare the measured R_{OO} trend with Xantheas's MP2 result only. The measured and calculated trends are quite similar in degree of curvature, which represents the relative importance of many-body potential energy terms as cluster size increases. The MP2 curve predicts convergence to the ordered ice value by $n=6$ or 7, while the experimental curve indicates a slightly more rapid convergence by $n=4$ or 5.

IV. TUNNELING SPLITTINGS

In order to account for all the features observed in the VRT spectrum of the water tetramer, it is convenient to develop a group theoretical description of the hydrogen bond formation–bond breaking processes, which generates a description of the quantum tunneling dynamics that is consistent with *ab initio* tunneling pathway calculations, and provides the vanishing integral properties that also rationalize other observations, such as the $K=2$ splittings (and the absence of such splittings in other K states). Such descriptions, employing permutation-inversion (PI) group theory[63] have been used successfully to rationalize the VRT spectra of several cluster systems wherein dynamical effects such as quantum tunneling are observable in the spectra, viz. the water dimer[64,65] and trimer,[15,37] the ammonia dimer,[19] and other complexes.[63] In many of these systems, nearly free rotation of the monomer constituents has given rise to experimental manifestations of all possible internal motions via tunneling splittings or energy level shifts.

A brief group theoretical analysis of the water tetramer tunneling dynamics was given in Ref. 16. However, since the structures of larger cyclic water clusters may be more rigid due to cooperative H-bonding effects and decreased H-bond strain (e.g., no evidence of tunneling involving breaking of hydrogen bonds was observed in the water pentamer FIR spectrum[17]), and since the connectivity of structurally degenerate and nodegenerate minima on the associated IPS becomes exponentially more complicated as the dimensionality grows, caution must be observed in rationalizing the origin of spectral splittings in these complex systems. In the following sections, three possible scenarios will be considered in order to account for the observed 5.6 MHz tunneling splittings: tunneling between degenerate IPS minima supporting the S_4 equilibrium structure, tunneling between nonstructurally equivalent IPS minima, and tunneling between degenerate upper state structures facilitated by excitation along a specific vibrational coordinate. Hypothetical energy level diagrams for these scenarios are shown in Fig. 6. The origin of the additional $K=2$ splittings will be addressed in Sec. V.

A. Degenerate tunneling

The dominant motion observed in water trimer VRT spectra is the ''flipping'' of one unbound proton from one side of the O–O–O plane, to the other (Fig. 1). In the trimer, this motion has been calculated[35] to lie below the cluster zero-point energy in $(H_2O)_3$ and very nearly so in $(D_2O)_3$. The facility of this motion accounts for the fact that homoisotopic trimers, with equilibrium C_1 geometric symmetry, are observed as vibrationally averaged symmetric tops with K being a good (or very nearly good) quantum number,[15] and for the fact that several low frequency torsional-mode VRT transitions have been observed,[31] analogous to the case of cyclopentane.[66] It is reasonable to begin any dynamical study of a cyclic water cluster by considering this motion. A single unbound proton flip yields a structure

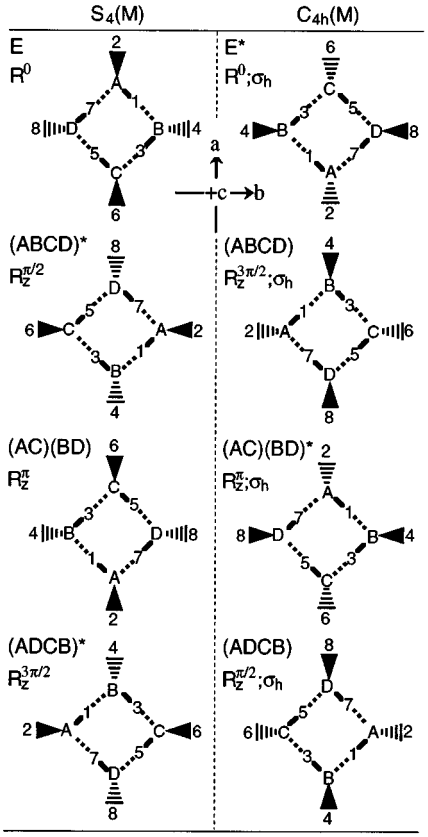

FIG. 7. The effects of the operations of the PI groups $S_4(M)$ (left column) and $C_{4h}(M)$ on the water tetramer. The labels A,B,C,D denote oxygen atoms and 1,2,...,8 label protons or deuterons. The cyclic permutation $(ABCD)$ is shorthand for $(ABCD)(1357)(2468)$, and so on. All operations preserve the bound and free status of the protons of each monomer. Each PI operation on the left-hand side can be represented by an equivalent rotation about the c principal axis of inertia (the z axis), while those on the right-hand side are represented by a similar rotation followed by a reflection through the O–O–O–O plane.

degenerate with the equilibrium configuration in water trimer or pentamer (or any odd numbered cyclic water cluster), but produces a nondegenerate tetramer structure. For an analogous motion to interconvert degenerate tetramer structures, simultaneous flipping of *all four* unbound protons across the O–O–O–O plane, analogous to the ammonia inversion, is required. In this section, we present a group theoretical rationalization of the VRT spectrum in terms of a proposed simultaneous flipping pathway between degenerate minima on the tetramer IPS [Fig. 6(A)]. Much of the group theoretical analysis presented here can also be of use in examining the other scenarios.

The largest molecular symmetry (MS) group of the water tetramer, without allowing for chemical bond breaking, consists of the 768 PI operations given by the direct product $S_4\times(S_2)^4\times\epsilon$, where S_4 and S_2 are the groups of all operations permuting four oxygen atoms and two protons (deuterons) respectively, and ϵ is the inversion group $\{E,E^*\}$. The effect of E^* is to invert all coordinates of the wave function through the cluster center of mass. The much larger complete nuclear permutation-inversion (CNPI) group is required for inclusion of breaking and reforming of chemical O–H bonds. Since the point group (S_4) of the equilibrium structure is of order 4, the 18-dimensional (monomer geometries fixed) tetramer IPS actually contains 192 structurally degenerate minima corresponding to the S_4 framework, which may or may not be separated by barriers penetrable by quantum tunneling. In practice, we seek the smallest subgroup of the MS group that is sufficient to explain the observables.

The smallest possible MS group of the water tetramer is $S_4(M)$, the PI group isomorphic to the point group S_4 which would describe a rigid, quasiplanar tetramer. The first column of Fig. 7 shows that each of the $S_4(M)$ PI operations rotate one labeled tetramer structure into another but do not permute the nuclear labeling. Since tunneling doublets are observed in the VRT spectra, it is necessary to include PI operations which interconvert two or more forms.

Inclusion of the PI operations which describe simultaneous flipping in water tetramer generates the subgroup $C_{4h}(M)$ of the MS group. The flipping operations are shown in the right-hand column of Fig. 7, and the character table of $C_{4h}(M)$ is given in Table IV. In what follows, it will be most convenient to work with the operations of $S_4(M)$ and generalize to the $C_{4h}(M)$ case as necessary. Since the character table of $S_4(M)$ is contained within that of $C_{4h}(M)$, the correlation of $S_4(M)$ states with $C_{4h}(M)$ states is easily obtained:

$$A=A_g\oplus B_u;\quad B=B_g\oplus A_u;$$
$$E_1=E_{1g}\oplus E_{2u};\quad E_2=E_{2g}\oplus E_{1u}. \tag{4}$$

Here we have chosen to individually label the separably degenerate E states of $S_4(M)$ and $C_{4h}(M)$, which are degenerate only by time (momentum) reversal symmetry. Each rovibronic state of the rigid tetramer then, should split into a doublet upon degenerate tunneling between S_4 IPS minima, with each level being labeled by an irreducible representation of $C_{4h}(M)$ as given in Eq. (4). The electric dipole selection rules $\Gamma_g\leftrightarrow\Gamma_u$ indicate that the VRT transitions should occur in tunneling doublets between any two states, with overall selection rules: $A_g\leftrightarrow A_u$, $B_g\leftrightarrow B_u$, $E_{1g}\leftrightarrow E_{2u}$, and $E_{2g}\leftrightarrow E_{1u}$. Nuclear spin statistical weights are determined from the number of H or D nuclear spin functions compatible with the ground state rovibronic wave functions. The results for $(H_2O)_4[(D_2O)_4]$ yield statistical weights 35[185] for A_g,A_u; 33[184] for B_g,B_u, and 30[180] for E_g,E_u states. Therefore the symmetry operations of the tetramer CNPI subgroup $C_{4h}(M)$ predict rovibronic transitions in doublets with nearly equal intensity. This is precisely what is observed in the VRT spectra for $K\neq 2$.

Equivalent rotations of the PI operations of $S_4(M)$ are also shown in Fig. 7. By considering the effect of each equivalent rotation on the Euler angles of the rigid tetramer, rotational state labels can be obtained. The character of an $S_4(M)$ operation as a function of the symmetric top K quantum number is given by

$$R_z^{\gamma}|J,\pm|K|,m\rangle=e^{\pm iK\gamma}|J,\pm|K|,m\rangle, \tag{5}$$

TABLE IV. The character table of $C_{4h}(M)$. The operations and character table of $S_4(M)$, a subgroup of $C_{4h}(M)$, are contained within the dotted lines. The irreducible representation labels of $S_4(M)$ are obtained by dropping the g subscript. The permutations $(ABCD)$ are shorthand for $(ABCD)(1357)(2468)$, where A,B,C,D label oxygen atoms, and where odd and even numbers label hydrogen-bonded and free protons or deuterons respectively (Fig. 7). In this group, the roles of donor and acceptor $D(H)$ atoms of one monomer are never reversed. The effects of the cyclic permutations are defined as in Ref. 63.

$C_{4h}(M)$	E	$(ABCD)^*$	$(AC)(BD)$	$(ADCB)^*$	$(ADCB)$	$(ABCD)$	E^*	$(AC)(BD)^*$
A_g	1	1	1	1	1	1	1	1
B_g	1	−1	1	−1	−1	−1	1	1
E_{1g}	1	$-i$	−1	i	i	$-i$	1	−1
E_{2g}	1	i	−1	$-i$	$-i$	i	1	−1
A_u	1	−1	1	−1	1	1	−1	−1
B_u	1	1	1	1	−1	−1	−1	−1
E_{1u}	1	i	−1	$-i$	i	$-i$	−1	1
E_{2u}	1	$-i$	−1	i	$-i$	i	−1	1

where ${R_z}^{\gamma}$ is a rotation of γ radians about the $z(C)$ axis. Since all equivalent rotations in $S_4(M)$ are about the molecule fixed z axis (Fig. 7), the rotational state labeling is independent of J. Rotational state labels under $S_4(M)$ are then: $K=\pm 4n$, A; $K=\pm(4n+2)$, B; $K=+(4n+1)$, E_1; $K=-(4n+1)$, E_2; $K=+(4n+3)$, E_2; $K=-(4n+3)$, E_1, where $n=0,1,2,...$ The correlation to $C_{4h}(M)$ states is again obtained from Eq. (4). From the character table, the total wave function of $(H_2O)_4$ must transform as either the B_g or B_u irreducible representations of $C_{4h}(M)$, while that of $(D_2O)_4$ must transform as either A_g or A_u, in order to obey the Pauli principle. With these labels, it is possible to determine the types of VRT transitions that can be observed assuming this tunneling scheme. Parallel (c-type) VRT spectra would be expected for transitions to upper vibrational states of $B=B_g\oplus A_u$ symmetry, while perpendicular (a-type) transitions would connect the ground state to states of $E=E_g\oplus E_u$ vibrational symmetry. Vibrational transitions to upper states of $A=A_g\oplus B_u$ symmetry would yield c-type rotational transitions originating from odd K states (E states) only. From these results it is clear that a parallel VRT spectrum with transitions allowed in all K manifolds is possible if the vibrational upper state transforms as either A_u or B_g in $C_{4h}(M)$ [B in $S_4(M)$].

Schütz and co-workers[67] have recently published symmetry assignments of tetramer normal mode harmonic frequencies (also calculated by Xantheas[38]). In that work, an A_u mode of $(D_2O)_4$ was predicted to lie at 142 cm^{-1}, with B_g modes at 77 and 247 cm^{-1}. The former two modes are predominantly torsional vibrations, i.e., in the flipping coordinates. Since *ab initio* harmonic vibrational frequencies are often too high by factors of 2 for these weakly bound systems, it seems unlikely that the spectrum measured in this work belongs to the lower frequency B_g mode, although we cannot explicitly rule out the possibility. Hence, we tentatively assign the present vibration to the calculated 142 cm^{-1} A_u torsional mode.

Larger subgroups of the MS group, describing other types of structural rearrangements, must also be considered. In the water trimer, ''donor'' or ''bifurcation'' tunneling, involving an exchange of bound and free protons of one water monomer in the ring structure accompanied by one or two flips on adjacent monomers, has been shown to lead to characteristic quartet splitting patterns in each vibration–rotation transition.[68] Simple extension of the group theoretical analysis which rationalizes this result in terms of degenerate tunneling leads to the result that each rovibrational level of a cyclic water cluster, $(H_2O)_n$, splits into $n+1$ levels which can be connected by n electric dipole transitions and might be expected to yield more complicated splitting patterns in the VRT spectrum. Inclusion of this donor tunneling motion into the tetramer MS group generates a group of order 240 (G_{240}), and we expect to see fivefold splitting patterns in the VRT spectra as a result of feasible bifurcation tunneling. Attempts to observe substructure in the measured VRT doublets have indicated no such effects. Neither was any evidence of bifurcation tunneling apparent in the VRT spectrum of water pentamer.[17] Therefore, if bifurcation tunneling is occurring in these larger systems, the spectral splittings must be less than the ~1 MHz experimental line width, at least insofar as the present data indicates.

The *ab initio* tetramer geometry optimizations of Schütz and co-workers[67] predict that an asymmetric cyclic structure (Fig. 8) with C_i point group symmetry lies just 0.86 kcal mol^{-1} higher in energy than the S_4 global minimum. A group theoretical analysis completely analogous to the above can be performed for that structure as well. Adopting the shorthand of Schütz *et al.*, where the unbound protons (deuterons) are described by ''u'' for above, ''d'' for below, and ''p'' for in the plane of the oxygens, the secondary minimum structure can be interconverted between four $\{uudd\}$ forms by the direct product of the PI operation (ABCD)(1357)(2468) with $\{E,E^*\}$, which forms a group of four PI operations isomorphic to $C_{2v},C_{2v}(M)$. The results of such an analysis predict that each VRT state of the rigid C_i tetramer should again split into two components of nearly equal intensity. Each A state in C_i correlates to $A_1\oplus B_2$, while each B level correlates to $A_2\oplus B_1$. The nuclear spin statistical weights are 65[365] for A_1 and A_2, and 63[364] for B_1 and B_2, for $(H_2O)_4$[$(D_2O)_4$]. Therefore, in this degenerate tunneling scheme involving a *twofold* flipping motion, doublets of nearly equal intensity are again predicted. Careful

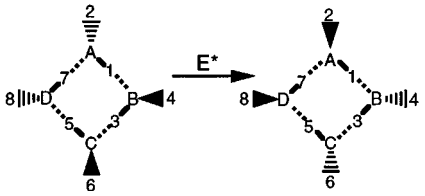

FIG. 8. A rearrangement of the $\{uudd\}$ low lying stationary point structure of the water tetramer with C_i symmetry. Schütz and co-workers (Ref. 68) calculate this structure to lie just 0.8 kcal mol^{-1} above the S_4 global minimum.

intensity measurements made on several of the tunneling doublet transitions in this spectrum reveal that the small differences in the predicted intensity patterns for the S_4 and C_i cases transcends the experimental capability. Fluctuations in the intensity measurements are too large to distinguish between these two cases at the present signal-to-noise level.

B. Nondegenerate tunneling

Wales[68] has examined several reaction paths producing tunneling splittings in small clusters and has found that, in addition to tunneling between degenerate structures, tunneling between nondegenerate structures separated by a relatively low barrier and having near resonant bound state energies, can lead to observable splittings in the VRT spectra. Figure 6(B) illustrates such a scheme, which is tantamount to observing two structures simultaneously, each undergoing a similar vibrational motion. Such a possibility cannot be explicitly ruled out in the present case, however it seems unlikely that such a scenario would lead to splittings which are independent of rotational quantum number, as nondegenerate wells on the IPS would almost certainly support differently spaced rotational state manifolds. Nevertheless, it is important to note that Wales and co-workers[69] have extensively probed *ab initio* IPS pathways for the water tetramer and find many more *nondegenerate* structural rearrangement pathways separated by first-order saddle points on the 16-*d* IPS than *degenerate* pathways.

Schütz and co-workers[67] predict small energy differences between a variety of torsional variants and the S_4 minimum energy structure. They find stationary points [CCSD(T)] calculations, aug-cc-pVDZ basis set) for $\{pppp\}$, $\{uuuu\}$, $\{uudd\}$, and $\{udpd\}$ tetramers, all lying within about 10% of the total binding energy (23.8 kcal mol^{-1}) of the $\{udud\}$ form. The $\{pppp\}$ stationary structure is the transition state for simultaneous flipping and was calculated to lie 2.9 kcal mol^{-1} higher than the S_4 structure, the others in the list above lying considerably closer. It is therefore conceivable that considerable sampling of non-S_4 minima takes place in the VRT dynamics of the water tetramer.

C. Vibrationally facilitated tunneling

In addition to the two possibilities discussed above, Schütz and co-workers[67] have pointed out that particular vibrational excitations can effectively lower the potential energy barriers separating degenerate upper state structures. For example, those authors found that excitation in the predicted 222 cm^{-1} B_u normal vibration leads to the $\{pppp\}$ stationary structure, the transition state for the simultaneous flipping motion discussed in Sec. IV A, effectively lowering the potential barrier to that motion. Interestingly, in such a case, the measured tunneling splitting would be a *direct* measure of the upper state VRT splitting, rather than a sum or difference as in case (A) and perhaps case (B) (Fig. 6). Measurement of the splitting would, therefore, provide a direct estimate of the effective barrier to simultaneous flipping. The group theoretical discussion given in Sec. IV A would apply in this case as well, producing the same selection rules, doublet splitting pattern and intensity ratios.

V. THE $K=2$ SPLITTINGS

The additional doublet splittings observed in the $K=2$ states (Table III and Fig. 3) are plotted in Fig. 4 as a function of both the lower and upper state rotational quantum number J. Figure 4 indicates that this splitting occurs in both the upper and lower vibrational states, since the splittings for P and R branches differ as a function of J. Previous experience with the water trimer[14,15] has shown that vibration–rotation coupling can lead to significant perturbations in the VRT spectra, even to the degree that the spectra are unassignable using standard rigid-rotor assumptions.[14] These perturbations, while not yet fully quantified, appear to arise from the fact that the internal torsional motions and overall rotational angular momentum can couple to produce both energy level splittings and/or shifts from the normal semirigid rotor pattern. Recent work by van der Avoird and co-workers has provided a satisfying rationalization of extra splittings in the 82 cm^{-1} $(H_2O)_3$ VRT spectrum in terms of kinetic coupling of bifurcation tunneling, flipping, and the overall rotation. Those splittings are quite similar to those observed in the tetramer data, in that they increase approximately as J^2 and are observed only in a limited subset of P- and R-branch transitions.

Efforts to interpret the complicated perturbations in the trimer spectra are ongoing and have included detailed reaction pathway calculations in order to assess the possible dynamics, and kinetic and potential energy couplings between them. It seems clear at this point that a fundamental understanding of the torsional motions and couplings in the trimer, along with similar reaction pathway calculations for the tetramer, will be a necessary precursor to understanding the origin of the $K=2$ water tetramer splittings.

VI. DISCUSSION

The rotational constants and symmetric top nature of the $(D_2O)_4$ spectrum reported here are in good agreement with theoretical predictions of an S_4 equilibrium water tetramer structure. Given previous experience with the water trimer and pentamer, however, it would not be unreasonable to expect cyclic, asymmetric equilibrium structures (e.g., the C_2 structure discussed above) to also exhibit symmetric rotor VRT spectra, due to facile flipping motions which effectively

average the out-of-plane coordinates. That the spectrum presented here is due to a symmetric top molecule is insufficient information to confirm which of the cyclic structures, calculated to be nearby in energy, is in fact the correct equilibrium ground state structure. Furthermore, the fact that the zero-point energy of the cluster may even be above the barrier to interconversion between two or more of the cyclic minima underscores the notion that it is the IPS of these complexes that is of primary significance, and not the measured structures themselves.

Observation of a cyclic tetramer is also consistent with results of previous studies of small water clusters. In molecular beam electric field deflection studies, Dyke and Meunter[70] showed that clusters larger than the dimer were not significantly deflected by strong electric field gradients, ostensibly indicating small permanent average dipole moments after considering the vibrational averaging effected by the flipping motions. The dipole moment of the S_4 tetramer is zero by symmetry, while simple vector models of the trimer and other cyclic tetramer forms yield vanishingly small moments. In a variety of low energy electron attachment experiments, Haberland and co-workers[71–73] were able to attach an electron to dipole bound states of $(H_2O)_n$ and $(D_2O)_n$ for every n except $n=4$, with small signals for $n=3$ and 5. Since the threshold dipole moment for electron attachment is roughly 1.8 D, they concluded that the tetramer dipole moment is below that limit. We note, however, that this conclusion relies on the assumption that the structures of the neutral and negative ion are not significantly different and that a number of different cluster structures may have been present in the supersonic expansion employed therein. Finally, Page[74] and co-workers observed infrared predissociation spectra of several small water clusters, finding distinct stretching frequencies for bound and free local mode OH stretches.

Observation of a perpendicular ($\Delta C=\pm 1$) spectrum, from which the C rotational constant could be determined, would significantly augment the data presented here. Recent work by Fellers and co-workers[75] has revealed such a spectrum near 510 cm^{-1} which is currently under analysis. With this information, the type of analysis recently carried out by Liu[30] for $(D_2O)_3$ might be used to gain further insight into hydrogen bond torsional motions in the tetramer, as well as a more realistic estimate of R_{OO}. The analysis of the Q-branch intensities in the present spectrum, however, is sufficient to bracket the C constant to a near planar oblate top value, $C\approx B/2$, consistent with theoretical predictions of quasiplanar equilibrium structure. Indeed, observation of Q-branch transitions with $J=K$ as high as 19 in a rotationally cold ($\sim$5 K) expansion alone confirms that the molecule is quite oblate.

While the experimental evidence is most consistent with a degenerate tunneling scheme analogous to those observed in other systems like the water dimer and trimer, the present data alone are insufficient to completely specify the dynamics responsible for the 5.6 MHz tunneling splittings. Neither can the data discriminate against a tunneling scheme like that discussed in Sec. IV C. The data do argue against a nondegenerate tunneling scheme, however, by the invariance of the measured tunneling splittings with respect to rotational energy. By the same argument, however, it is possible that the J-dependent $K=2$ splittings are a result of tunneling between nondegenerate structures. A complete exposition of nondegenerate tunneling possibilities along with a group theoretical treatment such as has been presented by Wales and co-workers[68] for the trimer would be of value in deciding the origin of that effect.

Much more experimental and theoretical work will be required to fully characterize the torsional dynamics in the water clusters studied to date. Even in the case of the water trimer, where recent work[76] has characterized more of the low frequency torsional motions, the picture of how these motions couple to the overall rotation of the cluster and to other intermolecular motions is still not quantitative. As in the case of the water dimer, where it is apparent that a fully coupled six-dimensional-calculation of the intermolecular bound states is necessary to fully describe the VRT dynamics, larger water clusters are also likely to defy a low dimensional analysis.

The interpretation of the vibrationally averaged structures of larger cyclic water clusters has provided insight into the relative magnitudes of many body forces in water. The exponential decrease in the interoxygen separation in the clusters, which approaches the ordered ice limit by $n=5$ or 6 is in reasonable agreement with the MP2 calculation of Xantheas,[38] which predicts that three-body interactions account for 18% of the total stabilization energy of the trimer and that three- and four-body interactions account for 24% and 2% of the tetramer energy, respectively. In their perturbative *ab initio* treatment, Chalasinski and co-workers[77] have provided insight into the nature of the three-body interaction forces in water trimer, noting that the principal contribution is from mutual polarization of the monomers resulting in deformations of the charge clouds (self-consistent field deformation). It is hoped that the VRT data will provide a route for quantifying the various interactions in the trimer and larger clusters once methods for calculating the eigenstates of those more complicated systems are developed. We note that Gregory and Clary[40] have recently achieved very impressive progress toward this end with the use of a diffusion Monte Carlo approach, reporting fully coupled 30-dimensional dynamics to near spectroscopic accuracy for the nodeless VRT states of the water hexamer.

In order to fully assess the questions surrounding the dynamics of this interesting system, it is clear that more data, in concert with further theoretical efforts, is necessary. To that end, searches for other intermolecular VRT spectra of $(H_2O)_n$ and $(D_2O)_n$ are presently underway, with the goals of completely mapping out the torsional subspaces, exploring the nontorsional dynamics, acquiring further structural data for cyclic water clusters, and measuring the structures and dynamics of larger water clusters. We hope that this work stimulates the requisite theoretical effort necessary to realize our goal of achieving a quantitative description of the forces and dynamics operative in small water clusters.

ACKNOWLEDGMENTS

This work was supported by the Experimental Physical Chemistry Program of the National Science Foundation under Grant No. CHE-9424482. R.J.S. is grateful to D. J. Wales for many helpful discussions.

[1] K. Liu, J. D. Cruzan, and R. J. Saykally, Science **271**, 877 (1996).
[2] G. T. Fraser, Int. Rev. Phys. Chem. **10**, 189 (1991).
[3] M. J. Elrod and R. J. Saykally, Chem. Rev. **94**, 1975 (1994).
[4] A. C. Belch and S. A. Rice, J. Chem. Phys. **86**, 5676 (1987).
[5] I. Ohmine, J. Phys. Chem. **99**, 6767 (1995).
[6] P. L. Moore-Plummer, J. Mol. Struct. **237**, 47 (1990).
[7] Z. Shi, S. Wei, J. V. Ford, and A. W. Castleman, Jr., Chem. Phys. Lett. **200**, 142 (1992).
[8] H. Tanaka, J. Chem. Phys. **101**, 10833 (1994).
[9] C. Y Lee, J. A. McCammon, and P. J. Rossky, J. Chem. Phys. **80**, 4448 (1984).
[10] M. M. Teeter, Proc. Natl. Acad. Sci. USA **81**, 6014 (1984).
[11] S. Neidle, H. M. Berman, and H. S. Shieh, Nature **288**, 129 (1980).
[12] R. C. Cohen and R. J. Saykally, J. Phys. Chem. **96**, 1024 (1992).
[13] N. Pugliano and R. J. Saykally, J. Chem. Phys. **96**, 1832 (1992).
[14] N. Pugliano, J. D. Cruzan, J. G. Loeser, and R. J. Saykally, J. Chem. Phys. **98**, 6600 (1993).
[15] K. Liu, J. G. Loeser, M. J. Elrod, B. C. Host, J. A. Rzepiela, and R. J. Saykally, J. Am. Chem. Soc. **116**, 3507 (1994).
[16] J. D. Cruzan, L. B. Braly, K. Liu, M. G. Brown, J. G. Loeser, and R. J. Saykally, Science **271**, 59 (1996).
[17] K. Liu, M. G. Brown, J. D. Cruzan, and R. J. Saykally, Science **271**, 62 (1996).
[18] M. J. Elrod, J. G. Loeser, and R. J. Saykally, J. Chem. Phys. **98**, 5352 (1993).
[19] J. G. Loeser, C. A. Schmuttenmaer, R. C. Cohen, M. J. Elrod, D. W. Steyert, R. J. Saykally, R. E. Bumgarner, and G. A. Blake, J. Chem. Phys. **97**, 4727 (1992).
[20] R. C. Cohen and R. J. Saykally, J. Chem. Phys. **98**, 6007 (1993).
[21] C. A. Schmuttenmaer, R. C. Cohen, and R. J. Saykally, J. Chem. Phys. **101**, 146 (1994).
[22] M. J. Elrod and R. J. Saykally, J. Chem. Phys. **103**, 933 (1995).
[23] E. H. T. Olthof, A. van der Avoird, and P. E. S. Wormer, J. Chem. Phys. **101**, 8430 (1994).
[24] M. J. Elrod, R. J. Saykally, A. R. Cooper, and J. M. Hutson, Mol. Phys. **81**, 579 (1994).
[25] M. J. Elrod, D. W. Steyert, and R. J. Saykally, J. Chem. Phys. **95**, 3812 (1991).
[26] M. J. Elrod, D. W. Steyert, and R. J. Saykally, J. Chem. Phys. **94**, 58 (1991).
[27] C. LeForestier, J. Chem. Phys. **101**, 7357 (1995).
[28] N. Pugliano and R. J. Saykally, Science **257**, 1937 (1992).
[29] K. Liu, J. G. Loeser, M. J. Elrod, J. Rzepiela, J. D. Cruzan, and R. J. Saykally, Faraday Trans. **97**, 35 (1994).
[30] K. Liu, M. G. Brown, M. R. Viant, J. D. Cruzan, and R. J. Saykally, Mol. Phys. (in press).
[31] S. Suzuki and G. A. Blake, Chem. Phys. Lett. **229**, 499 (1994).
[32] M. R. Viant, J. D. Cruzan, D. D. Lucas, K. Liu, M. G. Brown, and R. J. Saykally (unpublished).
[33] J. K. Gregory and D. C. Clary, J. Chem. Phys. **103**, 8924 (1995).
[34] E. H. T. Olthof, A. van der Avoird, and P. E. S. Wormer,J. Chem. Phys. (submitted).
[35] M. Schütz, T. Burgi, and S. Leutwyler, J. Chem. Phys. **99**, 5228 (1993).
[36] A. vanderAvoird, E. H. T. Olthof, and P. E. S. Wormer, J. Chem. Phys. (submitted).
[37] D. J. Wales, J. Am. Chem. Soc. **115**, 11180 (1993).
[38] S. S. Xantheas and T. H. Dunning, Jr., J. Chem. Phys. **99**, 8774 (1993).
[39] S. S. Xantheas, J. Chem. Phys. **100**, 7523 (1994).
[40] K. Liu, M. G. Brown, J. K. Gregory, C. Carter, D. C. Clary, and R. J. Saykally, Nature **381**, 501 (1996).
[41] D. Belford and G. Campbell, J. Chem. Phys. **86**, 7013 (1987).
[42] L. A. Burke, J. O. Jensen, J. L. Jensen, and P. N. Krishnan, Chem. Phys. Lett. **206**, 293 (1993).
[43] C. E. Dykstra, J. Chem. Phys. **91**, 6472 (1989).
[44] S. C. Farantos, S. Kapetanakis, and A. Vegiri, J. Phys. Chem. **97**, 12158 (1993).
[45] K. A. Franken, M. Jalaie, and C. E. Dykstra, Chem. Phys. Lett. **198**, 59 (1992).
[46] K. S. Kim, M. Dupuis, G. C. Lie, and E. Clementi, Chem. Phys. Lett. **131**, 451 (1986).
[47] R. Knochenmuss and S. Leutwyler, J. Chem. Phys. **96**, 5233 (1992).
[48] K. Laasonen, M. Parrinello, R. Car, C. Lee, and D. Vanderbilt, Chem. Phys. Lett. **207**, 208 (1993).
[49] B. J. Mihn, H. S. Kim, C. W. Yoon, and K. S. Kim, Chem. Phys. Lett. **176**, 41 (1991).
[50] D. J. Wales and I. Ohmine, J. Chem. Phys. **98**, 7245 (1993).
[51] D. J. Wales and I. Ohmine, J. Chem. Phys. **95**, 7257 (1993).
[52] C. J. Tsai and K. D. Jordan, J. Chem. Phys. **95**, 3850 (1991).
[53] C. J. Tsai and K. D. Jordan, J. Phys. Chem. **97**, 5208 (1993).
[54] C. J. Tsai and K. D. Jordan, Chem. Phys. Lett. **213**, 181 (1993).
[55] B. J. Mhin, S. J. Lee, and K. S. Kim, Phys. Rev. A **48**, 3764 (1993).
[56] G. A. Blake, K. B. Laughlin, R. C. Cohen, K. L. Busarow, D.-H. Gwo, C. A. Schmuttenmaer, D. W. Steyert, and R. J. Saykally, Rev. Sci. Instrum. **62**, 1693, 1701 (1991).
[57] R. C. Cohen, K. L. Busarow, Y. T. Lee, and R. J. Saykally, J. Chem. Phys. **92**, 169 (1990).
[58] K. Liu, R. P. Fellers, M. R. Viant, R. P. McLaughlin, M. G. Brown, and R. J. Saykally, Rev. Sci. Instrum. **67**, 410 (1996).
[59] D. R. Herriott and H. J. Schulte, Appl. Opt. **4**, 883 (1965).
[60] D. Kaur, A. M. de Souza, J. Wanna, S. A. Hammad, L. Mercorelli, and D. S. Perry, Appl. Opt. **29**, 119 (1990).
[61] J. D. Cruzan, M. R. Viant, D. Lucas, and R. J. Saykally (unpublished).
[62] K. S. Kim, B. J. Mhin, U. S. Choi, and K. Lee, J. Chem. Phys. **97**, 6649 (1992).
[63] P. R. Bunker, *Molecular Symmetry and Spectroscopy* (Academic, San Diego, 1979), Vol. 1.
[64] T. R. Dyke, J. Chem. Phys. **66**, 492 (1976).
[65] T. R. Dyke, K. M. Mack, and J. S. Muenter, J. Chem. Phys. **66**, 498 (1977).
[66] D. O. Harris, G. G. Engerholm, C. A. Tolman, A. C. Luntz, R. A. Keller, H. Kim, and W. D. Gwinn, J. Chem. Phys. **50**, 2438 (1969).
[67] M. Schütz, W. Klopper, and H.-P. Luthi, J. Chem. Phys. **103**, 6114 (1995).
[68] D. J. Wales, J. Am. Chem. Soc. **115**, 11191 (1993).
[69] D. J. Wales (private communication).
[70] T. R. Dyke and J. S. Muenter, J. Chem. Phys. **57**, 5011 (1972).
[71] M. Armbruster, H. Haberland, and H. G. Schindler, Phys. Rev. Lett. **47**, 323 (1981).
[72] H. Haberland, C. Ludewigt, H.-G. Schindler, and D. R. Worsnop, Surf. Sci. **156**, 157 (1985).
[73] H. Haberland, C. Ludewigt, H. Schindler, and D. R. Worsnop, J. Chem. Phys. **81**, 3742 (1984).
[74] H. Page, J. G. Frey, Y.-R. Shen, and Y. T. Lee, Chem. Phys. Lett. **106**, 373 (1984).
[75] R. F. Fellers *et al.* (unpublished).
[76] J. D. Cruzan, M. R. Viant, D. D. Lucas, L. B. Braly, and R. J. Saykally (unpublished).
[77] G. Chalasinski, M. M. Szczesniak, P. Cieplak, and S. Scheiner, J. Chem. Phys. **94**, 2873 (1991).